

**NANO EXPRESS**

**Open Access**

# InSb-added TiO<sub>2</sub> nanocomposite films by RF sputtering

Seishi Abe

## Abstract

This study investigates the preparation of InSb-added TiO<sub>2</sub> nanocomposite films by RF sputtering. The optical absorption spectra are obviously shifted to visible and near-infrared regions. High-resolution transmission electron microscopy indicates that sphere-shaped InSb nanocrystals with a size of about 15 nm are dispersed in a matrix. The X-ray diffraction result reveals that the matrix forms a phase mixture of TiO<sub>2</sub> and In<sub>2</sub>O<sub>3</sub>, which is also produced by decomposing the InSb during postannealing at 723 K. Therefore, the absorption shift is clearly due to quantum size effects of the InSb nanocrystals embedded in the wide-gap oxides TiO<sub>2</sub> and In<sub>2</sub>O<sub>3</sub>.

**Keywords:** TiO<sub>2</sub> nanocomposite, Band gap, RF sputtering

## Background

Quantum dot solar cells have attracted much attention because of their potential to increase conversion efficiency [1]. Specifically, the optical absorption edge of a semiconductor nanocrystal is often shifted due to quantum size effects. The optical band gap can then be tuned to an effective energy region for absorbing the maximum intensity of the solar radiation spectrum. Furthermore, quantum dots produce multiple electron–hole pairs per photon through impact ionization, whereas bulk semiconductor produces one electron–hole pair per photon.

A wide-gap semiconductor sensitized by semiconductor nanocrystals is a candidate material for such use. Wide-gap materials such as TiO<sub>2</sub> and ZnO can only absorb the ultraviolet (UV) part of the solar radiation spectrum. The semiconductor nanocrystal supports the absorption of visible (vis) and near-infrared (NIR) light. Up to now, various nanocrystalline materials (InP [2], CdSe [3], CdS [4,5], PbS [6], and Ge [7,8]) have been investigated as sensitizers for TiO<sub>2</sub>. Wide-gap semiconductor ZnO was also investigated, since the band gap and the energetic position of the valence band maximum and conduction band minimum of ZnO are very close to those of TiO<sub>2</sub> [9]. Most of these composite materials were synthesized through chemical techniques, although physical deposition, such as sputtering, is also useful. In addition, one-step synthesis of a composite thin film is

favorable for low-cost production of solar cells. Package synthesis requires a specific material design for each deposition technique, for example, radio frequency (RF) sputtering [10,11] and hot-wall deposition [12]. The present study proposes a new composite thin film with InSb-added TiO<sub>2</sub> produced by RF sputtering. InSb nanocrystals may exhibit relatively high absorption efficiency due to a direct band structure with 0.17eV [13] and an exciton Bohr radius of 65.5 nm [14]. According to the material design, based on differences in the heat of formation [10,11], InSb nanocrystals are thermodynamically stable in an TiO<sub>2</sub>, since Ti is oxidized more than InSb because the free energy of oxidation in InSbO<sub>4</sub>, which is a typical oxide of InSb, exceeds that of the TiO<sub>2</sub> [15,16]. In addition, nanocrystalline InSb dispersed in the oxide matrix may exhibit quantum size effects, due to the wide band-gap of 3.2 eV in TiO<sub>2</sub> with anatase structure [17]. However, it is difficult to forecast how the composite will be formed in the one-step synthesis, since the compound semiconductor, InSb, may have decomposed during the preparation process. In the current study, the composition of InSb-added TiO<sub>2</sub> nanocomposite film is varied widely to find a composite with vis-NIR absorption due to the presence of InSb nanocrystals embedded in the wide-gap oxide matrix.

## Methods

An InSb-added TiO<sub>2</sub> nanocomposite film was prepared by RF sputtering from a composite target. Specifically,

Correspondence: [abe@denjiken.ne.jp](mailto:abe@denjiken.ne.jp)  
Research Institute for Electromagnetic Materials, Sendai 982-0807, Japan

$5 \times 5 \text{ mm}^2$  InSb chips, which were cleaved from a 2-in diameter InSb (100) wafer, were set on a 4-in diameter ceramic  $\text{TiO}_2$  target. The chamber was first evacuated to a vacuum of  $1.5 \times 10^{-7}$  Torr. InSb-added  $\text{TiO}_2$  nanocomposite films were deposited on a Corning #7059 glass substrate (Norcross, GA, USA) cooled by water. The distance between the target and the substrate was kept constant at 73 mm. The total gas pressure of argon or argon with diluted oxygen was fixed at  $2.0 \times 10^{-3}$  Torr. RF power and deposition time were kept constant at 200 W and 60 min, and no RF bias was applied to the substrate. The InSb-added  $\text{TiO}_2$  nanocomposite films thus deposited were successively annealed at temperatures from 623 to 923 K in 50 K steps for 60 min in a vacuum to crystallize both InSb and  $\text{TiO}_2$ . The film was structurally characterized using X-ray diffraction (XRD, Rigaku RAD-X, Rigaku Corporation, Tokyo, Japan). The optical-absorption spectrum of the film was measured using UV-vis-NIR spectroscopy (Shimadzu UV3150, Nakagyo-ku, Kyoto, Japan), and the composition of the film was analyzed using energy-dispersion spectroscopy (EDAX Phoenix, NJ, USA), operating at 10 kV with standard samples of  $\text{MnTiO}_3$  to calibrate the analyzed results for elements Ti and O and with InSb for elements In and Sb. The nanoscale structure was observed using high-resolution transmission electron microscopy (HRTEM, Hitachi H-9000NAR, Hitachi, Ltd., Tokyo, Japan) operating at 300 kV. Ion milling was performed during sample preparation.

## Results and discussion

Figure 1 depicts the transmittance spectra of as-deposited InSb-added  $\text{TiO}_2$  thin films prepared in a pure argon atmosphere. The composition of InSb can be varied by employing different InSb chip numbers while

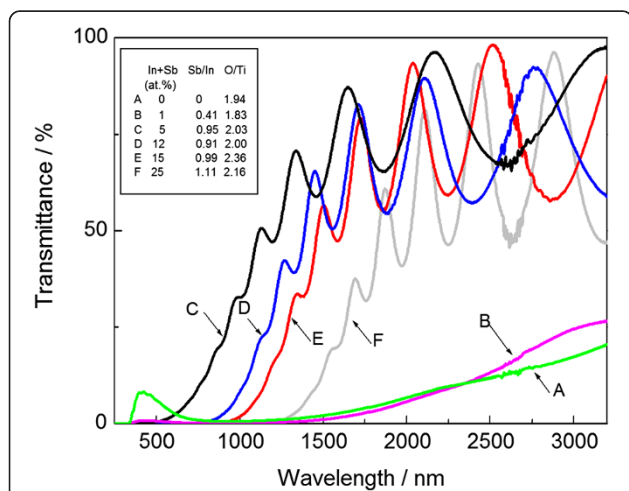
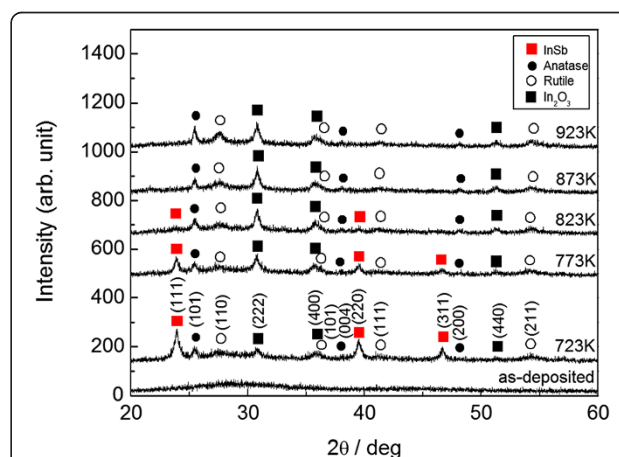


**Figure 1** Optical transmittance spectra of as-deposited InSb-added  $\text{TiO}_2$  thin films. Inset indicates EDS analysis results of In + Sb, Sb/In, and O/Ti.

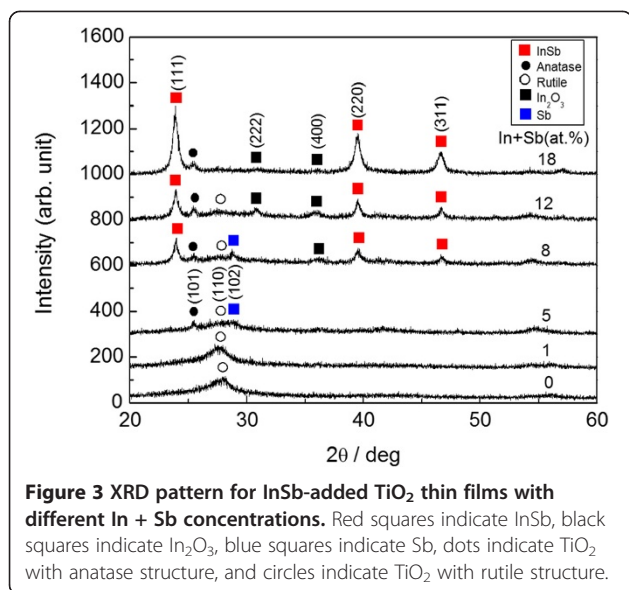
keeping almost stoichiometric InSb at concentrations exceeding 5 at.% (In + Sb). At 0 at.% (In + Sb), the optical absorption edge of  $\text{TiO}_2$  is observed at approximately 400 nm, with relatively less optical transparency in a wide range from UV to NIR. This weak transparency is due to the oxygen deficit in  $\text{TiO}_2$  with a composition ratio O/Ti of 1.94. A slight addition of 1 at.% also exhibits similar behavior, but further concentrations exceeding 5 at.% abruptly improve the transparency due to the excess oxygen in  $\text{TiO}_2$  with ratios O/Ti exceeding 2. This result suggests that the oxygen deficit in  $\text{TiO}_2$  is improved by adding InSb. In addition, the optical absorption edge shifts towards the longer wavelength region as the In + Sb content increases.

Figure 2 presents a typical XRD pattern of InSb-added  $\text{TiO}_2$  thin films annealed at different temperatures. In this case, the film was prepared in pure argon with an InSb chip number of 8 (15 at.% (In + Sb) in as-deposited film). The as-deposited film forms an amorphous structure, with XRD peaks of InSb,  $\text{In}_2\text{O}_3$ , and  $\text{TiO}_2$  (anatase and rutile) at a temperature of 723 K. The XRD peak of InSb tends to disappear at temperatures exceeding 823 K, beyond the melting point of 803 K, in InSb [18]. Thus, an annealing temperature of 723 K seems to be better to ensure the InSb phase stability.

Figure 3 presents the XRD patterns of InSb-added  $\text{TiO}_2$  thin films with different In + Sb concentrations. In this case, the film was deposited in a pure argon atmosphere and subsequently annealed at 723 K. Postannealing reduces the composition of In + Sb in most of the samples, typically from 25 at.% (as-deposited) to 18 at.% (annealed). There are no ternary or quaternary compounds in the patterns. At 0 and 1 at.% (In + Sb), only a rutile structure can be observed, with anatase structure

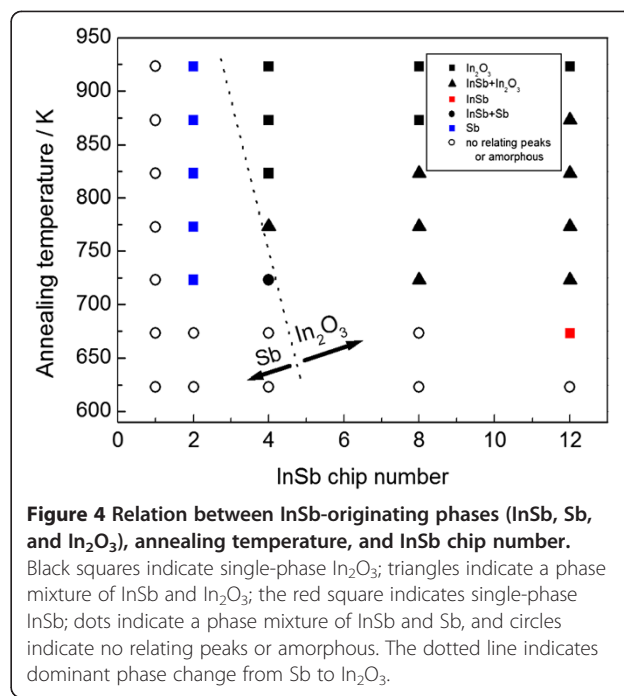


**Figure 2** XRD pattern for InSb-added  $\text{TiO}_2$  thin films with different annealing temperatures. Red squares indicate InSb, black squares indicate  $\text{In}_2\text{O}_3$ , dots indicate  $\text{TiO}_2$  with anatase structure, and circles indicate  $\text{TiO}_2$  with rutile structure.



and Sb peaks at 5 at.%, and with InSb and In<sub>2</sub>O<sub>3</sub> peaks at 8 at.%. Further addition of 12 at.% induces the disappearance of the Sb peak. In the experiment setup, two compounds, InSb and TiO<sub>2</sub>, are employed as the targets (i.e., metal Sb and In<sub>2</sub>O<sub>3</sub> compound are not used). In addition, the high transparency (Figure 1) strongly suggests that residual metal elements In and Sb are negligible in the as-deposited films with concentrations exceeding 5 at.%. Both Sb and In<sub>2</sub>O<sub>3</sub> are thus produced by decomposing the added InSb during postannealing.

The two phases, Sb and In<sub>2</sub>O<sub>3</sub>, are thus produced, due to decomposition of the added InSb during postannealing. These InSb-originating phases (InSb, Sb, and In<sub>2</sub>O<sub>3</sub>) are summarized in Figure 4 with respect to the InSb chip numbers and the annealing temperatures. The InSb phase crystallizes first at 623 K with an InSb chip number of 12 (25 at.% (In + Sb) in the as-deposited film). The Sb phase tends to appear with relatively small InSb chip numbers, less than four chips (12 at.% (In + Sb)), in contrast to the In<sub>2</sub>O<sub>3</sub> phase with its higher chip numbers and relatively high temperatures. The dominant phase changes from Sb to In<sub>2</sub>O<sub>3</sub> with respect to the InSb contents and annealing temperatures, although added InSb is almost stoichiometric, 2.7 at.% In + 2.6 at.% Sb with two InSb chips and 7.5 at.% In + 7.5 at.% Sb with eight chips, for example. Next, the composition is varied widely, with Ar and additional oxygen atmosphere, regardless of whether the TiO<sub>2</sub> phase, which is also contained in the composite, affects the difference in phase appearance (Sb and In<sub>2</sub>O<sub>3</sub>). Figure 5 depicts the compositional plane of the phase appearance in InSb-added TiO<sub>2</sub> thin films annealed at 723 K. The stoichiometric composition of TiO<sub>2</sub> with InSb is indicated by a dotted line. Single-phase TiO<sub>2</sub> appears in relatively low InSb concentrations. In particular, pure TiO<sub>2</sub> (In + Sb = 0)



has an oxygen deficit from stoichiometry in TiO<sub>2</sub>. This deficit causes low optical transparency over a wide wavelength range (Figure 1) at 0 at.% (In + Sb). In contrast, addition of InSb tends to provide excess oxygen from stoichiometric TiO<sub>2</sub>, in accordance with improving the transparency (Figure 1). InSb phase appears at 8 at.% (In + Sb), especially with In<sub>2</sub>O<sub>3</sub> exceeding 12 at.%. Further addition of oxygen provides an amorphous structure. Although the as-deposited films contain almost stoichiometric InSb, with the Sb/In ratio ranging from 0.9 to 1.2, postannealing induces sublimation of Sb with the ratio less than 0.9 as indicated by green, yellow, and red colors. Such an Sb deficit is seen not only in the In<sub>2</sub>O<sub>3</sub> with InSb and TiO<sub>2</sub> (circle), but also in the Sb with InSb and TiO<sub>2</sub> (square). Hence, the difference in phase appearance (Sb and In<sub>2</sub>O<sub>3</sub>) (Figure 4) seems to be independent of the compositional deviation from stoichiometry in a binary In-Sb system. According to the phase diagram of the In-Sb-O ternary system [19], the binary In-Sb system is in equilibrium with In<sub>2</sub>O<sub>3</sub>. A tie-line between the two phases (In<sub>2</sub>O<sub>3</sub> and In-Sb system) indicates that the oxygen concentration dominates the phase appearance in the binary system. Specifically, relatively high oxygen content provides Sb with an InSb phase, even with a nominal Sb deficit from stoichiometric InSb. This suggestion is consistent with the present result. Sb with an InSb phase appears at relatively high oxygen concentrations exceeding 61 at.%, and less oxygen is needed to provide In<sub>2</sub>O<sub>3</sub> with an InSb phase. It is therefore found that the difference in phase appearance (Sb and In<sub>2</sub>O<sub>3</sub>) (Figure 4) is due to the different inclusions of oxygen. In these results, the composite containing Sb does

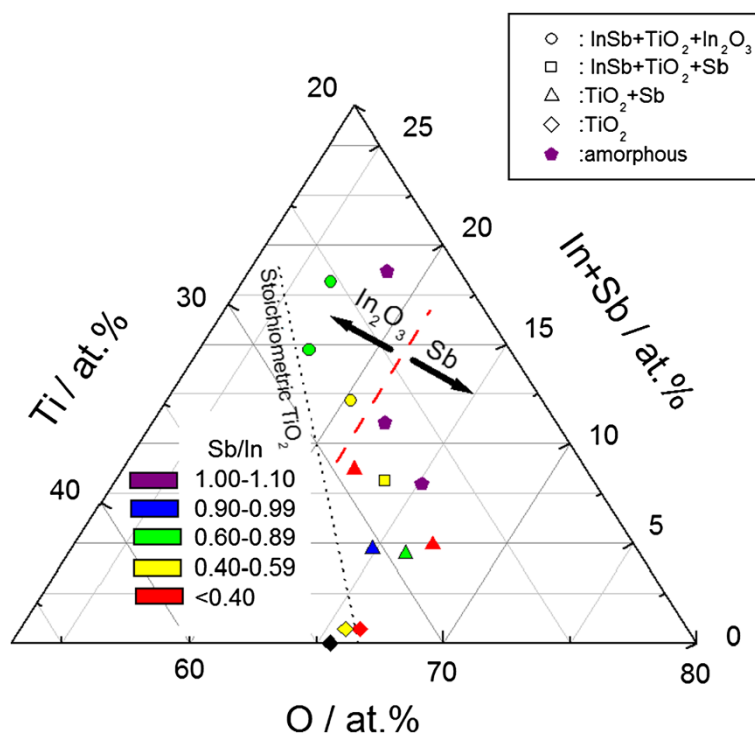
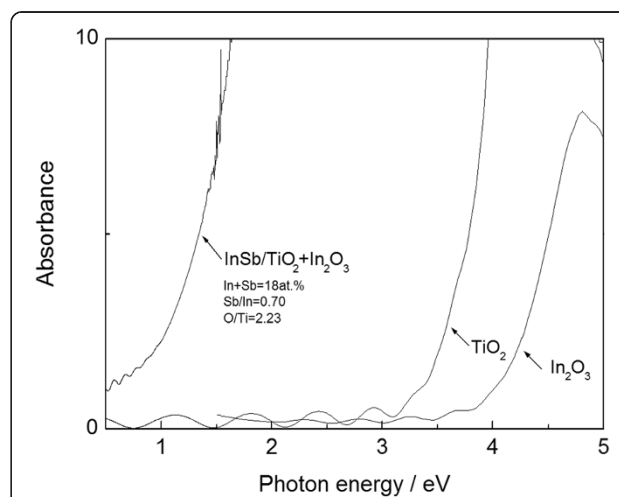


**Figure 5** Compositional plane of phase appearance in InSb-added TiO<sub>2</sub> thin films. Dots indicate a phase mixture of InSb, TiO<sub>2</sub>, and In<sub>2</sub>O<sub>3</sub>; squares indicate a phase mixture of InSb, TiO<sub>2</sub>, and Sb; triangles indicate a phase mixture of TiO<sub>2</sub> and Sb; rhombuses indicate single-phase TiO<sub>2</sub>; and pentagons indicate amorphous. Violet indicates an Sb/In ratio of 1.00 to 1.10; blue indicates 0.90 to 0.99; green indicates 0.60 to 0.89; yellow indicates 0.40 to 0.59; and red indicates less than 0.40.

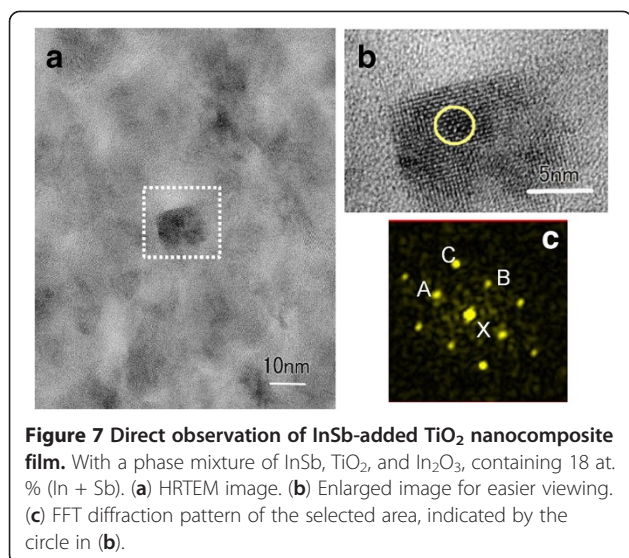
not achieve the present objective, since the residual Sb reduces the transparency. To avoid the inclusion of Sb, the sputtering target needs a different setup, such as excess In or less oxygen in the composite target, made of ceramic TiO<sub>2</sub> with InSb chips. A composite with InSb and single-phase TiO<sub>2</sub> cannot be obtained in the current study. However, the carrier mobility of the phase mixture of TiO<sub>2</sub> and In<sub>2</sub>O<sub>3</sub> exceeds that of the pure TiO<sub>2</sub> [20]. Thus, the inclusion of In<sub>2</sub>O<sub>3</sub> is considered to be useful for the current interest.

Figure 6 depicts a typical optical absorption spectrum for composite film with InSb, TiO<sub>2</sub>, and In<sub>2</sub>O<sub>3</sub>. For comparison, the absorption spectra of TiO<sub>2</sub> and In<sub>2</sub>O<sub>3</sub> are also presented in the figure. The absorption edge in both TiO<sub>2</sub> and In<sub>2</sub>O<sub>3</sub> appears in the UV range, while the composite film containing 18 at.% (In + Sb) exhibits an obvious shift to the vis-NIR range, thus absorb a desirable energy region for high conversion efficiency [21]. The composite film contains Sb deficit in InSb with a ratio Sb/In of 0.7. Hence, the actual concentration of InSb compound is estimated to be 15 at.%, assuming an Sb reacts fully to form InSb compound. The film also contains excess oxygen in TiO<sub>2</sub> with a ratio O/Ti of 2.23. The excess oxygen and the decomposed In may react to form In<sub>2</sub>O<sub>3</sub>. The analyzed oxygen content is enough just to form stoichiometric TiO<sub>2</sub> with an estimated concentration of 76 at.% and In<sub>2</sub>O<sub>3</sub> with 8 at.%. An

HRTEM image of the composite film is presented in Figure 7a. The slightly dark sphere-like nanocrystals are clearly dispersed, with a size of approximately 15 nm. The selected area (dotted line) is enlarged in Figure 7b for easier viewing. Fast Fourier transform (FFT) analysis of the region



**Figure 6** Typical optical absorption spectra of InSb-added TiO<sub>2</sub> composite film. With a phase mixture of InSb, TiO<sub>2</sub>, and In<sub>2</sub>O<sub>3</sub>, containing 18 at.% (In + Sb).



(circle in Figure 7b) reveals the details of the local structure in the nanocrystal. Figure 7c presents the corresponding FFT diffraction pattern, which can be indexed to cubic InSb. The spots labeled A, B, and C correspond to crystal faces of (110), (1-10), and (200) in the cubic InSb, with plane widths of 0.452, 0.466, and 0.330 nm, respectively. The angles labeled A-X-B, A-X-C, and B-X-C are 89°, 46°, and 43°. The standard data (JCPDS 6–208) indicates a plane width of 0.458 nm at both (110) and (1-10), and 0.324 nm at (200), with an angle of 90° for A-X-B and 45° for both A-X-C and B-X-C. The analysis results are close to the standard data. The observed grain is thus found to be cubic InSb nanocrystal. Therefore, InSb-added TiO<sub>2</sub> nanocomposite film produces a composite with InSb nanocrystals dispersed in a multiphase matrix composing TiO<sub>2</sub> and In<sub>2</sub>O<sub>3</sub>. The mean grain size of the InSb nanocrystals is estimated to be 18 nm using Scherrer's formula [22] in XRD peak fitting. This size is nearly the same as that of the observed InSb nanocrystals. This is small enough to exhibit the quantum size effects because of the exciton Bohr radius of 65.5 nm in InSb [14]. Furthermore, the ground state transition of electron–hole pairs in the semiconductor nanocrystal is calculated by the following formula [23,24]:  $E = E_g + (\hbar\pi)^2 / 2\mu R^2 - 1.8e^2 / 4\pi \epsilon \in \infty R$ , where  $E_g$  is the bulk band gap,  $\hbar$  is the reduced Planck constant,  $\mu$  is the reduced mass of an electron–hole pair,  $R$  is the effective Bohr radius,  $e$  is the electron charge, and  $\epsilon \infty$  is the background dielectric constant of InSb. Hence, the ground state transition of the InSb nanocrystals is calculated to be 0.78 eV, which corresponds well to the onset absorption containing 18 at.% (In and Sb) (Figure 6). Therefore, the optical absorption shift is obviously due to quantum size effects of the InSb nanocrystals embedded in the multiphase matrix, TiO<sub>2</sub> and In<sub>2</sub>O<sub>3</sub>.

InSb-added Al-oxide thin film, which is a similar composite containing InSb nanocrystals, produces a mean grain size of 8 nm during postannealing at 723 K, with similar concentrations of 9.5 at.% In and 13.5 at.% Sb [25]. The present result provides InSb nanocrystals of nearly twice this size. In addition, no inclusion of In<sub>2</sub>O<sub>3</sub> is seen in the InSb-added Al-oxide thin films, while this does appear in the present study (Figures 2 and 3). These different results are probably due to the difference in the free energy of reaction between the two oxides, TiO<sub>2</sub> and Al<sub>2</sub>O<sub>3</sub> [16]. Specifically, Al<sub>2</sub>O<sub>3</sub> with its smaller free energy of reaction is thermodynamically more stable than TiO<sub>2</sub>. InSb-added Al-oxide thin films also exhibit a narrower size distribution in the InSb nanocrystals compared with that of the SiO<sub>2</sub> matrix [26], whose free energy of reaction is close to that of the TiO<sub>2</sub>. The thermodynamic stability of the matrix may affect the aggregation of the InSb nanocrystals during postannealing, although the size distribution of the InSb nanocrystals dispersed in the multiphase matrix, TiO<sub>2</sub> and In<sub>2</sub>O<sub>3</sub>, is not estimated here, due to a difficulty of finding InSb nanocrystals in the HRTEM image containing three kinds of crystals, InSb, TiO<sub>2</sub>, and In<sub>2</sub>O<sub>3</sub>.

The present results indicate that InSb-added TiO<sub>2</sub> nanocomposite films provide a composite with InSb nanocrystals embedded in a multioxide matrix composing TiO<sub>2</sub> and In<sub>2</sub>O<sub>3</sub> and exhibiting vis-NIR absorption due to quantum size effects of the InSb nanocrystals. One-step synthesis of a composite thin film therefore has potential for low-cost production of next-generation solar cells.

## Conclusions

InSb-added TiO<sub>2</sub> nanocomposite films have been proposed as candidate materials for quantum dot solar cells. It should be pointed out that composite thin films with InSb nanocrystals dispersed in a multiphase matrix composing TiO<sub>2</sub> and In<sub>2</sub>O<sub>3</sub> appear in a restricted composition range from 12 to 18 at.% (In + Sb), because of compositional variation. The optical absorption edge shifts toward the vis-NIR range, favorably absorbing a desirable energy region for high conversion efficiency. A HRTEM image indicates that the composite thin film contains spherical InSb nanocrystals with a size of approximately 15 nm. This size is sufficiently small to exhibit quantum size effects. InSb-added TiO<sub>2</sub> nanocomposite films also produce In<sub>2</sub>O<sub>3</sub>, due to decomposition of the added InSb during postannealing. The electrical properties are not studied at all in the present study. However, the photocurrent of the composite may be enhanced by including In<sub>2</sub>O<sub>3</sub>, since the carrier mobility of the phase mixture of TiO<sub>2</sub> and In<sub>2</sub>O<sub>3</sub> is higher than that of the pure TiO<sub>2</sub>. Therefore, a multioxide matrix of TiO<sub>2</sub> and In<sub>2</sub>O<sub>3</sub> with InSb nanocrystals should be useful for next-generation solar cells.

#### Competing interests

The author declares that there are no competing interests.

#### Author information

SA is a group leader of the Research Institute for Electromagnetic Materials.

#### Acknowledgments

The present work was supported by a Grant-in-Aid for Scientific Research from the Japan Society for the Promotion of Science (No. 24360295). The author gratefully acknowledges the valuable comments of President T. Masumoto (Research Institute for Electromagnetic Materials (DENJIKEN), Sendai, Japan). The author is also grateful to Mr. N. Hoshi (DENJIKEN) for assisting in the experiments.

Received: 19 April 2013 Accepted: 30 May 2013

Published: 7 June 2013

#### References

- Nozik AJ: Quantum dot solar cells. *Phys E* 2002, **14**:115–120.
- Zaban A, Micic OI, Gregg BA, Nozik AJ: Photosensitization of nanoporous TiO<sub>2</sub> electrodes with InP quantum dots. *Langmuir* 1998, **14**:3153–3156.
- Liu D, Kamat PV: Photoelectrochemical behavior of thin CdSe and coupled TiO<sub>2</sub>/CdSe semi-conductor films. *J Phys Chem* 1993, **97**:10769–10773.
- Weller H: Quantum sized semiconductor particles in solution in modified layers. *Ber Bunsen-Ges Phys Chem* 1991, **95**:1361–1365.
- Zhu G, Su F, Lv T, Pan L, Sun Z: Au nanoparticles as interfacial layer for CdS quantum dot-sensitized solar cells. *Nanoscale Res Lett* 2010, **5**:1749–1754.
- Hoyer P, Könenkamp R: Photoconduction in porous TiO<sub>2</sub> sensitized by PbS quantum dots. *Appl Phys Lett* 1995, **66**:349–351.
- Chatterjee S, Goyal A, Shah I: Inorganic nanocomposites for next generation photovoltaics. *Mater Lett* 2006, **60**:3541–3543.
- Abe S, Ohnuma M, Ping DH, Ohnuma S: Anatase-dominant matrix in Ge/TiO<sub>2</sub> thin films prepared by RF sputtering method. *Appl Phys Exp* 2008, **1**:095001.
- Yang W, Wan F, Chen S, Jiang C: Hydrothermal growth and application of ZnO nanowire films with ZnO and TiO<sub>2</sub> buffer layers in dye-sensitized solar cells. *Nanoscale Res Lett* 2009, **4**:1486–1492.
- Ohnuma S, Fujimori H, Mitani S, Masumoto T: High-frequency magnetic properties in metal-nonmetal granular films. *J Appl Phys* 1996, **79**:5130–5135.
- Abe S: Formation of Nb<sub>2</sub>O<sub>5</sub> matrix and vis-NIR absorption in Nb-Ge-O thin film. *Nanoscale Res Lett* 2012, **7**:341.
- Abe S: One-step synthesis of PbSe-ZnSe composite thin film. *Nanoscale Res Lett* 2011, **6**:324.
- Little CL, Sella DG: Temperature dependence of the energy band gap of InSb using nonlinear optical techniques. *Appl Phys Lett* 1985, **46**:986–988.
- Lin MC, Chen PY, Su IW: Electrodeposition of zinc telluride from a zinc chloride-1-ethyl-methylimidazolium chloride molten salt. *J Electro Soc* 2001, **10**:c653.
- Band AJ, Oarsons R, Jordan J: *Standard potentials in aqueous solution*. New York: Taylor & Francis; 1985:70–83.
- Kubachevski O, Alcock CB: *Metallurgical Thermochemistry*. Oxford: Pergamon; 1979.
- Tang H, Prasad K, Sanjine's R, Schmid PE, Levy F: Electrical and optical properties of TiO<sub>2</sub> anatase thin films. *J Appl Phys* 1994, **75**:2042.
- Sharma X, Ngai N, Chang A: The In-Sb system. *J Phase Equilibria* 1989, **10**:657–664.
- Kobayashi J, Itoh S: Thermodynamic study on indium-antimony-oxygen system with respect to recycling of rare metals from compound semiconductors. *J Japan Inst Metals* 2008, **72**:763–768.
- Chen Y, Zhou X, Zhao X, He X, Gu X: Crystallite structure, surface morphology and optical properties of In<sub>2</sub>O<sub>3</sub>-TiO<sub>2</sub> composite thin films by sol-gel method. *Materials Science and Engineering B* 2008, **151**:179–186.
- Loferski JJ: Theoretical considerations covering the choice of the optimum semiconductor for photovoltaic solar energy conversion. *J Appl Phys* 1956, **27**:777–784.
- Scherrer P: Bestimmung der Größe und der inneren Struktur von Kolloidteilchen mittels Röntgenstrahlen. *Göttinger Nachrichten* 1918, **2**:98–100.
- Brus LE: A simple model for the ionization potential, electron affinity, and aqueous redox potentials of small semiconductor crystallites. *J Chem Phys* 1983, **79**:5566–5571.
- Giessen H, Flugel B, Mohs G, Peyghambarian N, Sprague JR, Micic OI, Nozik AJ: Observation of the quantum confined ground state in InP quantum dots at 300K. *Appl Phys Lett* 1996, **68**:304–306.
- Usui H, Abe S, Ohnuma S: InSb/Al-O nanogranular films prepared by RF sputtering. *J Phys Chem C* 2009, **113**:20589–20593.
- Zhu K, Shi J, Zhang L: Preparation and optical absorption of InSb microcrystallites embedded in SiO<sub>2</sub> thin films. *Solid State Commun* 1998, **107**:79–84.

doi:10.1186/1556-276X-8-269

Cite this article as: Abe: InSb-added TiO<sub>2</sub> nanocomposite films by RF sputtering. *Nanoscale Research Letters* 2013 **8**:269.

Submit your manuscript to a SpringerOpen<sup>®</sup> journal and benefit from:

- Convenient online submission
- Rigorous peer review
- Immediate publication on acceptance
- Open access: articles freely available online
- High visibility within the field
- Retaining the copyright to your article

Submit your next manuscript at ► [springeropen.com](http://springeropen.com)